Langmuir

Article

pubs.acs.org/Langmuir

Quantum Dots Self Assembly Based Interface for Blood Cancer Detection

Aditya Sharma,[†,‡] Gajjala Sumana,[†] Sameer Sapra,[‡] and Bansi Dhar Malhotra*[,†,§,⊥]

[†]Department of Science & Technology Centre on Biomolecular Electronics, Biomedical Instrumentation Section, CSIR-National Physical Laboratory, New Delhi 110012, India

[‡]Department of Chemistry, Indian Institute of Technology Delhi, New Delhi 110016, India

[§]Department of Biotechnology, Delhi Technological University, Delhi 110042, India

[⊥]Centre for NanoBioengineering & SpinTronics, Chungnam National University, 220 Gung-Dong, Yuseong-Gu, Daejeon 305764, South Korea

ABSTRACT: Results of the studies related to fabrication of sensitive electrochemical biosensor using an interface based on quantum dots (QDs) self-assembly is reported. The QDs assembly is sought to provide improved fundamental characteristics to the electrode interface in terms of electroactive surface area, diffusion coefficient, and electron transfer kinetics. This QDs modified electrode has been utilized to serve as a transducer surface for covalent immobilization of chronic myelogenous leukemia (CML) specific probe oligonucleotide, designed from the BCR-ABL fusion gene. The electrochemical characteristics of this biosensor toward various designed synthetic oligonucleotides reveal a significant enhancement in its mismatch discrimination capability compared to the biosensing assay without QDs under similar experimental conditions. The sensing characteristics of this biosensor offer a potential for detection of target oligonucleotide at a concentration as low as 1.0 pM. Furthermore, the PCR-amplified CML-positive patient samples with various BCR-ABL transcript ratios can be electrochemically distinguished from healthy samples, indicating promising application of the QDs based biosensor for clinical investigations.

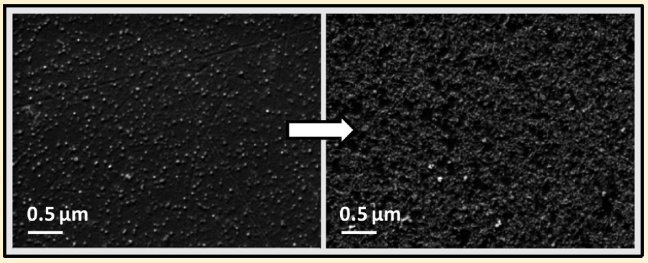

1. INTRODUCTION

Chronic myelogenous leukemia (CML) is a hematological disorder characterized by increased proliferation of the granulocytic cell-lines without the loss of their inherent characteristics to differentiate.[1] Consequently, the peripheral blood cell profile shows an increased number of granulocytes and their immature precursors, including occasional blast cells. CML is known to be caused by a single, specific genetic mutation. More than 90% of the cases[2] result from a cytogenetic aberration known as the Philadelphia chromosome arising from t(9;22)(q34;q11) reciprocal translocation, leading to generation of the BCR-ABL oncogene.[3] The resultant fused gene codes for a protein of 210 kDa (p210 BCR-ABL), constitutively chimeric tyrosine kinase.[4] Typically, tyrosine kinase regulates proliferation and survival of normal cells. However, its hyperactivity disrupts this fine balance, leading to production of cells that are endowed with proliferative advantages such as blocking of apoptosis, genome instability, and suppression of normal hematopoiesis, thereby providing the pathogenesis for CML.[2] The CML inevitably regresses and acquires lethality in absence of curative treatment, necessitating diagnosis in the chronic phase wherein patients are usually asymptomatic or have mild symptoms for the disease.

Current clinical diagnostic techniques of CML include chromosome analysis, fluorescence in situ hybridization, flow cytometry, and RT-PCR.[5,6] Quantitative competitive PCR can be used for monitoring patients with CML after bone marrow transplantation as low or decreasing BCR-ABL expression constitutes a good prognostic factor. However, the results obtained are dependent on the quality of the RNA sample. Moreover, majority of the assays are laboratory-based, labor-intensive, expensive, and are time-consuming, which limits their application as routine diagnostic tool resulting in delay of the prognosis and decision-making for treatments.[5] Therefore, efforts are being made to develop bioassays that require only a few handling steps, making the point of care analysis and diagnosis of CML possible at an early stage. In this context, the electrochemical biosensors have recently attracted significant interest in clinical diagnostics due to their high sensitivity, portability, rapid monitoring, and compatibility with the microfabrication technology.[7−14]

The performance of a biosensor critically depends on biomolecular immobilization onto a suitable matrix. The interfacing of a biomolecule with a nanomaterial may perhaps lead to the tailoring of a wide range of functional hybrid materials for biosensor applications. Current research direction

Received: April 17, 2013
Revised: May 30, 2013
Published: May 31, 2013

dx.doi.org/10.1021/la401431q | *Langmuir* 2013, 29, 8753−8762

Scheme 1. Steps Involved in the Fabrication of pDNA/CdTe/AS/ITO Bioelectrode

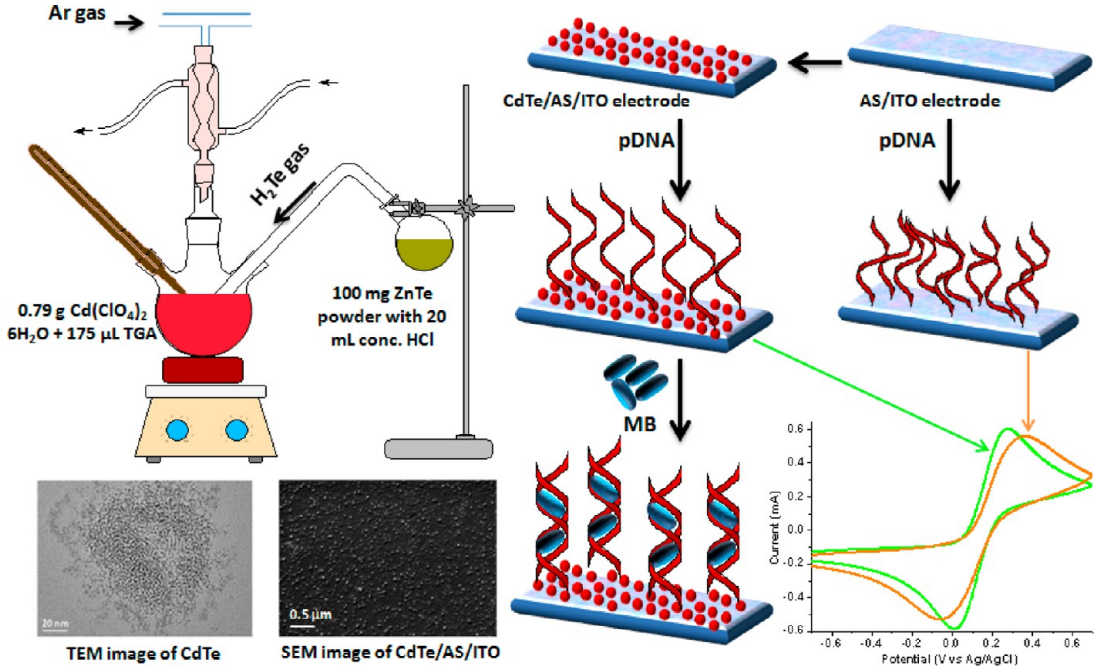

is to use these hybrid materials to obtain improved sensing characteristics that may lead to the evolution of advanced biosensors. It has been suggested that quantum dots can be employed as functional materials for electrochemical sensing, owing to their high reactivity and the ability to participate in charge-transfer.[13−16] Recently, Hua et al. have used QDs as the immobilization substrate to study conformational switching of an aptamer using electrochemical method.[15] A sensitive electrochemical aptasensor based on CdSe QDs is reported by Li et al., wherein ionic centers of the QDs are found to play a major role in amplification of the signal.[16]

Keeping in view potential of the QDs towards the development of electrochemical biosensing assays, we have utilized these nanoentities as a transducer surface for the fabrication of CML specific DNA biosensor. In our previous study, we have used the Langmuir−Blodgett (LB) film of QDs for electrochemical transduction of DNA hybridization for CML detection.[13] Although the LB technique allows transfer of orderly arranged particulates onto substrate, but the process is time-consuming and the particles carry *van der Waals* and ionic interactions among them. In the present studies, the CdTe QDs are self-assembled onto ITO substrate using silane as a cross-linker that permits covalent bonding of the particles with the substrate. The methodology adopted here exhibits inherent advantages in terms of simplicity and less time consumption for the bioelectrode preparation. The larger surface area of three-dimensional structure of QDs as compared to that of the two-dimensional structure of the silane self-assembled monolayer is found to result in decreased barrier for diffusion of the redox species, thereby contributing to improved kinetics compared to that observed in the absence of QDs. The analysis performed with clinical patient samples and comparative studies with gold standard (RT-PCR) indicate high potential of this smart biosensor as an add-on technique for initial screening of CML.

2. MATERIALS AND METHODS

2.1. Chemicals and Oligonucleotides. All of the chemicals used are of analytical grade and have been obtained from Sigma−Aldrich, India. Amine terminated CML specific probe oligonucleotide sequence identified from BCR-ABL gene of Philadelphia chromosome (UID No. 12859844) and all other designed sequences have been procured from Sigma−Aldrich, Milwaukee, WI and are reported elsewhere.[13] The solutions of probe and target oligonucleotides are prepared in Tris-EDTA buffer (1 M Tris−HCl, 0.5 M EDTA) of pH 8.0 and stored at −20 °C. The reagents have been prepared in deionized water (Millipore, 18.0 MΩ·cm) and the solutions and glassware are autoclaved prior to use.

2.2. Characterization. Ultraviolet−visible absorption studies have been carried out using Phoenix−2200DPCV spectrophotometer. The fluorescence spectrum has been recorded using a luminescence spectrometer (Edinburgh Instrument, F900) equipped with a xenon lamp. Fourier transform infrared (FT−IR) measurements have been taken in the specular reflectance mode using a Perkin−Elmer Spectrum BX II spectrophotometer. The FTIR signal is obtained by averaging 32 scans at the resolution of 1 cm^{-1}. The morphological characterization has been carried out using a high−resolution transmission electron microscope (HR−TEM, Tecnaii−G2F30 STWIN) and scanning electron microscope (SEM, VP-EVO MA10, Carl Zeiss). The electrochemical characterization has been conducted on an Autolab Potentiostat/Galvanostat (Eco Chemie, Netherlands) using a three−electrode system with ITO as the working electrode, Ag/AgCl as the reference electrode and platinum as counter electrode, in phosphate buffer saline (PBS, 100 mM, pH 7.4, 0.9% NaCl) containing 5 mM $[Fe(CN)_6]^{3-/4-}$.

2.3. Preparation of CdTe Quantum Dots. The synthesis of thioglycolic acid (TGA) capped CdTe-QDs has been accomplished by the reported procedure.[17] Briefly, 2.5 mmol TGA (175 µL) is added to the aqueous solution of cadmium perchlorate (19 mM, 125 mL) under continuous stirring. The pH of the solution adjusted to 11.5 and is deaerated by argon bubbling for about 1 h in a three−necked flask. Under stirring, H_2Te gas (generated by the reaction of 0.5 mmol of Al_2Te_3 lumps with 15 mL of 0.5 M H_2SO_4) is passed through the solution together with a slow nitrogen flow until the solution becomes reddish−brown. The solution is allowed to reflux at 100 °C for about 4 h under open air conditions. The nanocrystals are washed with acetone and redispersed in water to obtain the concentration of 5 mg/mL.

2.4. Self-Assembly of CdTe onto ITO Electrode. Prior to self-assembled monolayer (SAM) formation, ITO coated glass substrates (0.5 × 2 cm^2) are hydrolyzed with $H_2O_2/NH_4OH/H_2O$ solution (1:1:5, v/v) for 30 min at 80 °C. The hydrolyzed ITO substrates are

dx.doi.org/10.1021/la401431q | *Langmuir* 2013, 29, 8753−8762

immersed into 0.2% (v/v) aqueous solution of (3-aminopropyl)-trimethoxysilane (AS) for about 2 h for SAM formation, followed by washing with water to remove any unbound AS molecules.[18] Subsequently, the silanized ITO substrates are dipped overnight in CdTe solution containing *N*-ethyl-*N*′-(3-dimethylaminopropyl) carbodiimide (EDC; 0.2 M) and *N*-hydroxy succinimide (NHS; 0.05 M). The presence of EDC/NHS leads to the activation of carboxylic groups on TGA capped CdTe QDs, rendering them to self-assemble onto AS/ITO electrode via amide bond formation.[19] The electrodes are subsequently rinsed with water to remove any unbound CdTe particles, followed by drying in air.

2.5. Fabrication of pDNA/CdTe/AS/ITO Bioelectrode. The immobilization of amine terminated probe DNA onto CdTe/AS/ITO electrodes has been performed for bioelectrode fabrication (Scheme 1). For this purpose, 30 μL of pDNA (1 μM) is spread onto each electrode surface (0.5 cm^2 surface area) that is incubated for 6 h in a humid chamber at room temperature (25 °C) to allow amide bond formation with TGA capped CdTe quantum dots.[19] The fabricated pDNA/CdTe/AS/ITO bioelectrodes are repeatedly rinsed with TE buffer (pH 8.0) to remove any unbound pDNA present on the surface, and stored at 4 °C after drying. To accomplish the hybridization, these bioelectrodes are subjected to incubation with different concentrations of target DNA.

2.6. Processing and Gel Electrophoresis of Clinical Samples. The extraction of RNA from the patient's blood samples, its reverse transcription to complementary DNA (cDNA), and the processing have been performed as previously reported.[14] These aliquots of samples are subjected to sonication at 24 kHz frequency for different time intervals using ultrasonic cleaner, (Vibronics Pvt. Ltd., Mumbai, India) to break long DNA strands into smaller fragments.[13,14] Fragmentation of cDNA has been evaluated by agarose gel electrophoresis (3% in TAE buffer 1X) for which probe DNA (22 bases) and hybrid DNA (22 base pairs) are used as the molecular weight markers. Prior to loading, 6X tracking dye (1 μL per 5 μL sample) containing bromophenol blue and glycerol is added to the sample, and the gel is allowed to run at a constant voltage of 65 V for 50 min. Following electrophoresis, the gel is stained with methylene blue solution (MB; 0.002%) and the electrophoretic bands and distributions are visualized under white light and photographed by a digital camera.

3. RESULTS AND DISCUSSION

The formation of quantum dots has been confirmed via normalized absorption and photoluminescence spectra of aqueous suspension of CdTe nanocrystals (Figure 1). Appearance of absorbance maxima at 540 nm corresponding to the first exciton peak (curve i), and fluorescence maxima at 580 nm (curve ii) indicate the formation of CdTe quantum dots. The average size of the particles, as calculated via first exciton peak, is about 3.2 nm.[20] High resolution transmission electron microscopic images have also been recorded, which indicate that the particles exhibit size distribution ranging from 3 to 4.5 nm (inset Figure 1).

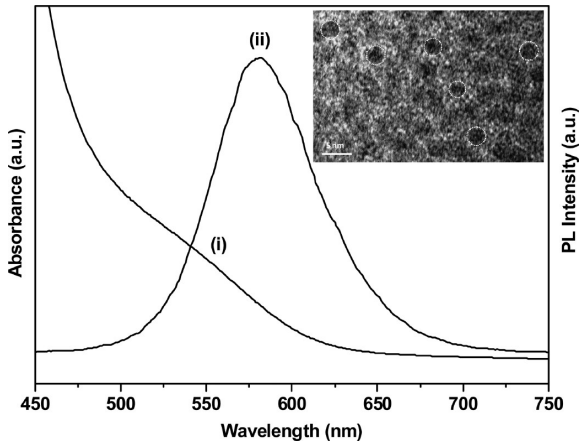

Figure 1. (i) Normalized absorption spectrum and (ii) photoluminescence spectrum of CdTe-QDs. Inset shows HRTEM image of the particles at a magnification of 5 nm.

FT−IR spectroscopic studies have been carried out at each step of the surface modification to verify the bioelectrode fabrication (Figure 2). The FT−IR spectrum of AS/ITO

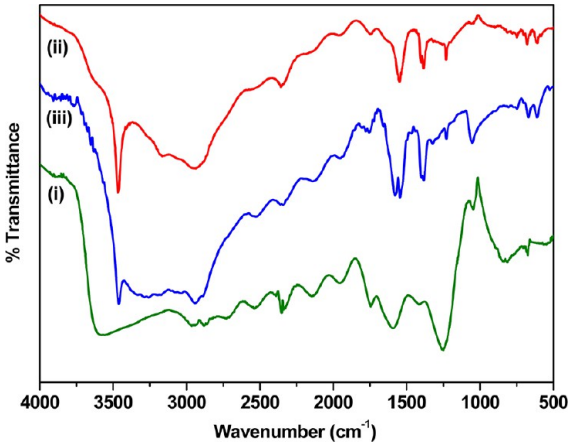

Figure 2. FT−IR spectra of (i) AS/ITO electrode, (ii) CdTe/AS/ITO electrode, and (iii) pDNA/CdTe/AS/ITO bioelectrode.

electrode (curve i) displays prominent peaks at 675 and 814 cm^{-1} for Si−O symmetric stretching and bending modes respectively, 1047 cm^{-1} for Si−O−Si stretching, 1592 cm^{-1} corresponding to NH_2 deformation in 1° amine, 2352 cm^{-1} for Si−C stretching, and a band in the range from 1174 to 1366 cm^{-1} corresponding to Si−O−C asymmetric stretching vibration.[21,22] The appearance of these characteristic peaks indicates self-assembly of AS onto ITO substrate via siloxane bond formation. However, in the FT−IR spectrum of CdTe/AS/ITO electrode (curve ii), the additional peaks seen at about 609, 750, 1386, and 1405 cm^{-1}, corresponding to C−S stretch and COO^- symmetric stretch and O−H bend, respectively, and a broad band in the range from about 3000 cm^{-1} to 2700 cm^{-1} corresponding to O−H stretch in carboxylic acids, may be correlated to the presence of TGA capped CdTe onto the electrode surface.[23] The shifting of peak from 1593 to 1551 cm^{-1}, corresponding to NH deformation in 2° amide and the appearance of a small shoulder in the range from 1650 cm^{-1} to 1640 cm^{-1} pertaining to C═O stretch in the 2° amide (amide I band), confirms covalent attachment of the CdTe-QDs to AS-SAM. Further, in the case of pDNA/CdTe/AS/ITO bioelectrode (curve iii), the additional sharp peaks are found at 1054 and 1580 cm^{-1} corresponding to P−O−C antisymmetric stretching vibration and NH_2 deformation in 1° amine, respectively. These peaks may perhaps be due to presence of the phosphodiester backbone and nucleoside residues indicating immobilization of pDNA onto the CdTe/AS/ITO electrode surface.[24]

The morphological changes at the electrode, arising as a result of surface modification, have been examined using scanning electron microscopic technique and the results are displayed in Figure 3. As can be seen (Figure 3, panel i), the AS film on the ITO surface is homogeneous, which paves the way

dx.doi.org/10.1021/la401431q | *Langmuir* 2013, 29, 8753−8762

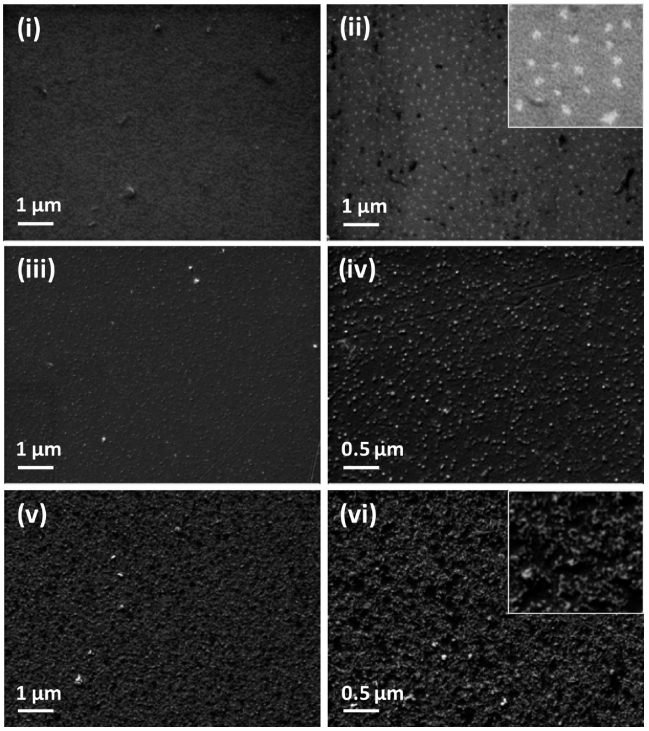

Figure 3. SEM images of (i) AS/ITO electrode, (ii) pDNA/AS/ITO bioelectrode, (iii and iv) CdTe/AS/ITO electrode, and (v and vi) pDNA/CdTe/AS/ITO bioelectrode.

for uniform distribution of the CdTe-QDs onto the electrode surface (Figure 3, panels iii and iv). When CdTe/AS/ITO electrode is incubated with pDNA, the spherical appearance is found to be diminished and the fibrous structures are observed (Figure 3, panels v and vi). This transformation from spherical to fibrous morphology may be attributed to the immobilization of pDNA on the QDs surface. Further, from the SEM images of both the bioelectrodes, it can be seen that pDNA/CdTe/AS/ITO bioelectrode has a more compact arrangement of pDNA compared to that of the pDNA/AS/ITO bioelectrode (Figure 3, panel ii).

The electrochemical behavior of the electrodes and bioelectrodes has been studied in the potential range from −0.6 to 0.75 V at the scan rate 30 mV/s, using cyclic voltammetric technique. Figure 4A shows a cyclic voltammogram of the AS/ITO electrode that exhibits a sharp oxidation peak at 0.27 V with a peak current (I_p) value of 8.96×10^{-4} A (curve i). After the self-assembly of the CdTe QDs onto AS/ITO electrode, a decrease in I_p value to 6.62×10^{-4} A is observed (curve ii). This may be attributed to the semiconducting nature of the QDs, resulting in slower electron transfer from the electrolyte to the electrode surface. The I_p value further decreases to 5.96×10^{-4} A upon the immobilization of pDNA on the CdTe/AS/ITO electrode (curve iii), suggesting formation of the insulating layer on the electrode surface leading to the decreased electron transfer. The control experiment has been carried out by immobilizing pDNA onto the AS/ITO electrode using glutaraldehyde as a cross-linker (curve iv). Apart from a sharp decrease in the I_p value to 5.62×10^{-4} A, a significant shift in peak potential as compared to that of pDNA/CdTe/AS/ITO electrode is observed (curve v). This increased mean value of peak separation indicates that a larger overpotential is required to achieve the same rate of electron transfer, and it can be correlated with slower rate of electron transfer across the interface.[25]

The CV studies have been conducted at various potential scan rates (υ, 10 to 300 mV/s) to investigate the interfacial kinetics on the electrodes and bioelectrodes surface. As the scan rate is increased, the anodic and cathodic peaks of electrodes and bioelectrodes are found to move in opposite directions, suggesting the redox process to be quasi-reversible. The linear variation of peak potential as a logarithmic function of scan rate, in the range from 10 to 300 mV/s, is depicted in Figure 4B (panel i). Using Laviron's equations, the value of electron transfer coefficient (α), for n number of electrons, has been determined from the slope of two straight lines with anodic and cathodic slopes of $2.303RT/(1-\alpha)nF$ and $-2.303RT/\alpha nF$, respectively. The charge transfer rate constant (k_s) has been calculated using eq 1:[26]

$$\ln K_s = \alpha(1-\alpha) + (1-\alpha)\ln\alpha - (RT/nF\upsilon) - \alpha nF\Delta E_p/RT \quad (1)$$

It is revealed that the CdTe/AS/ITO electrode exhibits a higher k_s value (0.0458 s^{-1}) as compared to that of the AS/ITO electrode (0.0278 s^{-1}). This enhanced k_s value at the surface of AS/ITO electrode after modification with CdTe QDs clearly indicates that the electronic structure and the surface physicochemistry of QDs contribute to the increased electron transfer. Using the above equation, k_s values have been determined for each electrode after immobilization of pDNA. As can be seen in Table 1, the k_s value significantly decreases for both electrodes after pDNA immobilization. However, the pDNA/CdTe/AS/ITO bioelectrode exhibits faster electron transfer kinetics. This may perhaps be due to oriented immobilization of the biomolecules on the CdTe/AS/ITO electrode surface that provides an easier path for the transfer of electrons from the redox species to the electrode and vice versa. On the basis of the linear slope of the anodic peak currents on the square root of potential sweep rates (Figure 4B, panel ii), it is clear that the ions transport from bulk to the electrode surface occurs exclusively by diffusion.[27] Diffusion coefficient (D) is determined by a concentration gradient of $[Fe(CN)_6]^{3-/4-}$ ions between bulk and interface and can be calculated via the Randles−Sevick equation:[28]

$$I_p = (2.69 \times 10^5)\alpha^{1/2}n^{3/2}ACD^{1/2}\upsilon^{1/2} \quad (2)$$

where C is the molar concentration of $[Fe(CN)_6]^{3-/4-}$, and A is the electrode surface area that is immersed in the electrolyte solution (0.5 cm^2). The D value for CdTe/AS/ITO electrode is found to be greater than that of the AS/ITO electrode. The electroactive surface area (A_e) of the modified electrode is further obtained by using the calculated diffusion coefficient and the Randles−Sevcik equation:[29]

$$A = S/(2.99 \times 10^5)n^{3/2}CD^{1/2} \quad (3)$$

where S is the slope obtained from the linear regression of I_p versus $\upsilon^{1/2}$. The A_e value calculated for both the AS/ITO and CdTe/AS/ITO electrodes are 1.14 and 1.17 mm^2, respectively, indicating that a close electrical contact exists between CdTe-QDs and the silane modified ITO electrode.[30]

For a surface-controlled process, the surface concentration of ionic species can be estimated using eq 4:[26]

dx.doi.org/10.1021/la401431q | Langmuir 2013, 29, 8753−8762

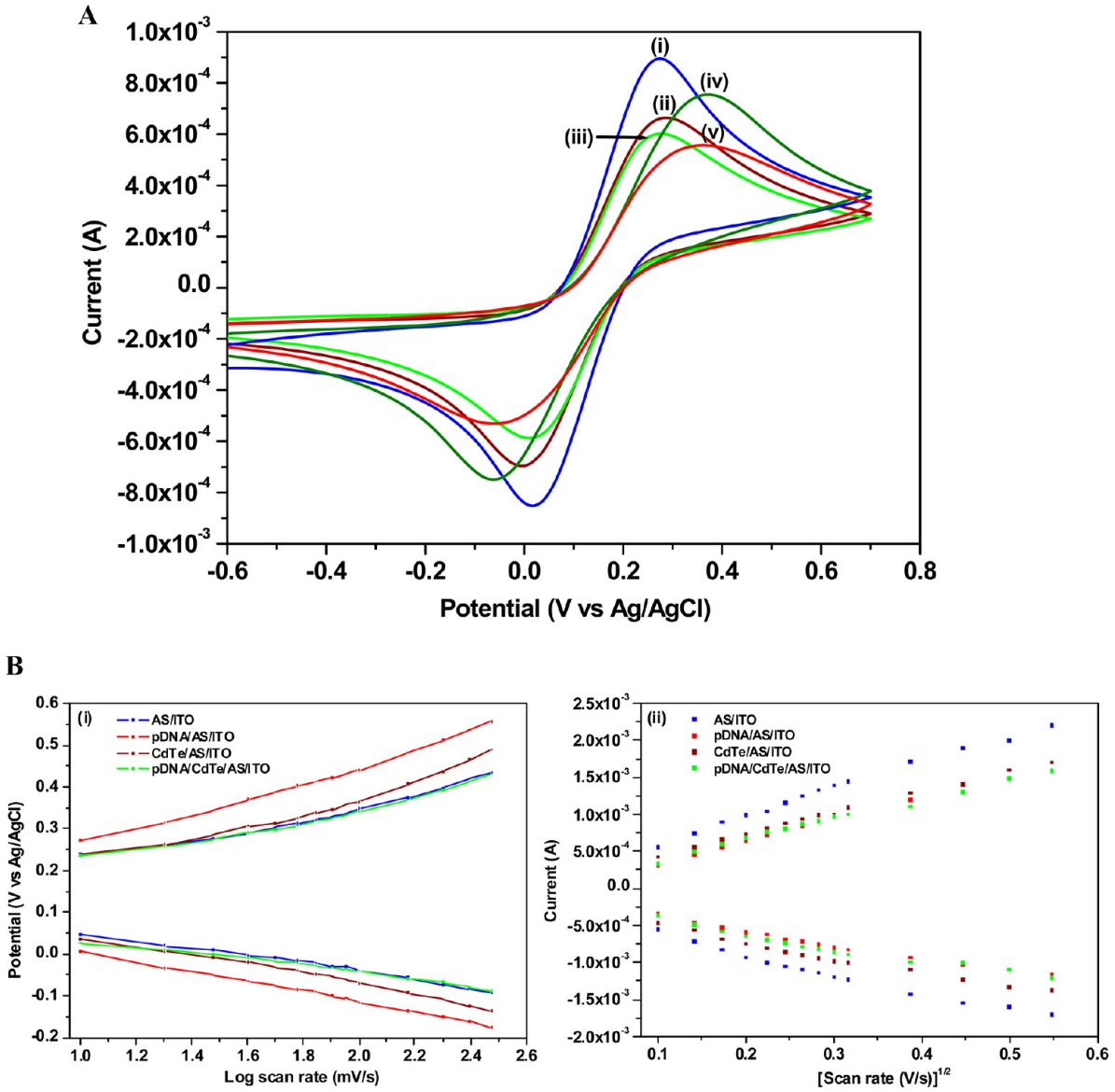

Figure 4. (A) Cyclic voltammogram of (i) AS/ITO electrode, (ii) CdTe/AS/ITO electrode, (iii) pDNA/CdTe/AS/ITO bioelectrode, (iv) Glu-AS/ITO electrode, and (v) pDNA/AS/ITO bioelectrode, in PBS (50 mM, pH 7.4, 0.9% NaCl) solution containing 5 mM $[Fe(CN)_6]^{3-/4-}$. (B) Cyclic voltammetric variation of (i) potential with log of scan rate and (ii) current with square root of scan rate.

Table 1. Values of Kinetic Parameters Calculated for Modified Electrodes

name of the electrode	electron transfer coefficient (α)	charge transfer rate constant (k_s; s^{-1})	diffusion coefficient (D; $cm^2\ s^{-1}$)	electroactive surface area (A_e; mm^2)	average surface concentration (Γ; mol cm^{-2})	anodic peak current (I_{pa}; A)
AS/ITO	0.5898	0.0278	6.93×10^{-11}	1.14	5.72×10^{-8}	8.96×10^{-4}
CdTe/AS/ITO	0.5969	0.0458	7.29×10^{-11}	1.17	6.59×10^{-8}	6.61×10^{-4}
pDNA/AS/ITO	0.6170	0.0057	1.48×10^{-11}	1.53	2.48×10^{-8}	5.56×10^{-4}
pDNA/CdTe/AS/ITO	0.6291	0.0168	2.02×10^{-11}	1.22	3.01×10^{-8}	5.95×10^{-4}

$$I_p = n^2F^2\upsilon A\Gamma(4RT)^{-1} \quad (4)$$

where, I_p is peak current, and Γ is the average surface concentration of the electrode redox substance (mol cm^{-2}). The enhanced Γ value for CdTe/AS/ITO electrode as compared to that of the AS/ITO electrode can be correlated to high surface coverage of immobilized probe molecules onto nanostructured CdTe/AS/ITO electrode[31] compared to that on the smoother surface for AS/ITO electrode. This is mainly attributed to the zero dimensional nanostructure of QDs providing high surface to volume ratio, resulting in an enhanced quantity of chemisorbed pDNA on the CdTe modified electrode, as observed in SEM studies.

Differential pulse voltammetry (DPV) has been used to investigate the electrochemical response of the fabricated pDNA/CdTe/AS/ITO bioelectrode for detection of CML

dx.doi.org/10.1021/la401431q | Langmuir 2013, 29, 8753−8762

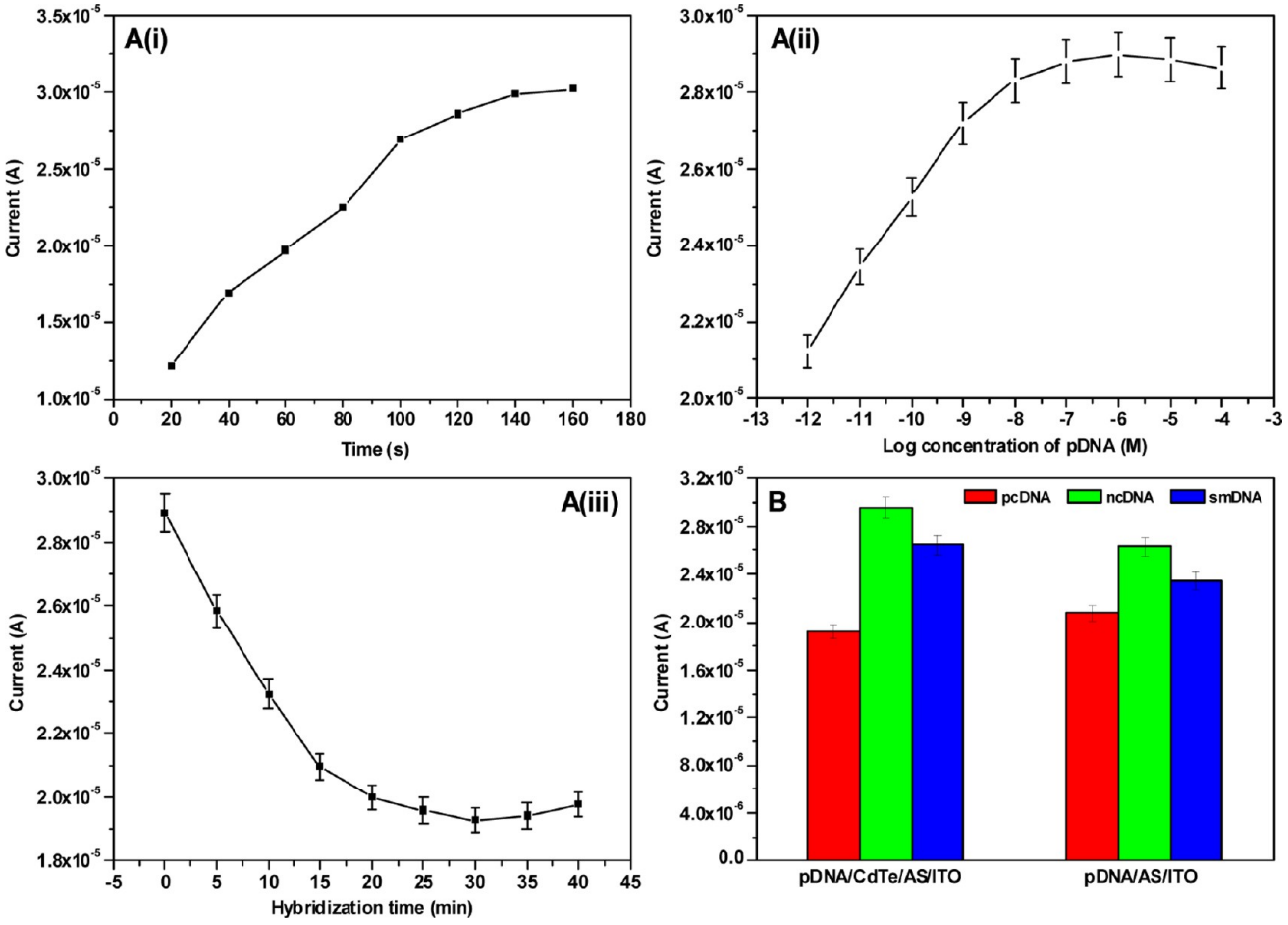

Figure 5. (A) (i) Response current of the pDNA/CdTe/AS/ITO bioelectrode (100 μM of pDNA immobilized) on interaction with MB at varying time intervals, (ii) MB reduction current value for the pDNA/CdTe/AS/ITO bioelectrode as a logarithmic function of probe DNA concentration, and (iii) variation in MB reduction current value for the pDNA/CdTe/AS/ITO bioelectrode after hybridization with 1 μM pcDNA for different time intervals. (B) Histogram showing variation in MB reduction current value for pDNA/CdTe/AS/ITO and pDNA/AS/ITO bioelectrodes after incubation with 1 μM concentration of pcDNA, ncDNA, and smDNA.

using MB as a redox hybridization indicator. It has been found that an incubation time of 120 s is sufficient for interaction of the MB molecules with probe DNA. The response time of the biosensor, measured as the time to reach ~95% of the maximum change in response on injection of methylene blue (20 μM) in the electrolyte solution (Phosphate buffer saline, pH 7.4), is found to be about 120 s (Figure 5A (panel i)). Response time in the present work depends on the diffusion rate of MB across the interface to get reduced to leuco-methylene blue. MB is used as an electrochemical marker that can be reduced at the electrode surface by two electrons to leucomethylene blue.[32] The reduction is facilitated by the oxidation of unpaired nucleoside bases of single-stranded DNA that are unavailable after hybridization, leading to retardation of the corresponding signal.[33] As the oligonucleotide chain is composed of amine rich nucleoside residues, it is expected that the presence of free QDs on the bioelectrode surface may lead to chemisorption of the complementary target molecules, thereby providing the false positive signal. To minimize the competition of the hybridization event with non-specific adsorption of the complementary target, a study to optimize the probe DNA concentration has been performed. As shown in Figure 5A (panel ii), by increasing the amount of pDNA from 1 pM to 1 μM, higher DPV signals are achieved, while from 1 to 100 μM, the electrochemical signal is leveled off. For further studies, 1 μM concentration of the pDNA is used, presuming that complete immobilization is achieved at this concentration.

Since analytical performance of the nucleic acid is directly related to its ability to recognize the target oligonucleotide, it is essential to optimize the time required for the hybridization to take place. Figure 5A (panel iii) shows the influence of incubation time (0−40 min) on the differential pulse voltammetric response of the system in the presence of 1 μM complementary target DNA, using MB as a redox hybridization indicator. The DPV signal, pertaining to reduction of MB, decreases with increasing hybridization time up to 30 min, after which it saturates. Therefore, this incubation time has been used in further experiments considering that maximum extent of hybridization is accomplished in this duration.

In order to investigate the specificity, hybridization studies have been performed with the complementary target (pcDNA), single-base mismatch (smDNA), and noncomplementary DNA (ncDNA) sequences. Figure 5B shows comparison of the peak currents of these three target DNA sequences to that of the background (corresponding bioelectrode). Equal concentration of each oligonucleotide (1 μM) is subjected to hybridization with the probe DNA immobilized on the bioelectrode surface, and the corresponding signal of MB reduction current value is recorded. In the presence of smDNA, the electrochemical

dx.doi.org/10.1021/la401431q | Langmuir 2013, 29, 8753−8762

signal of the pDNA/CdTe/AS/ITO bioelectrode is found to decrease by about 9.0%, while in the presence of perfect matched target DNA (pcDNA), the signal decreases by as much as about 34.5%, approximately 4 times the decrease achieved in the presence of smDNA. It may be noted that no significant variation in current signal is observed with ncDNA sequence. As explained earlier, the significant current difference obtained for pcDNA (Δ is about 19.6 μA) is attributed to the fact that interaction between the MB molecules and nucleoside residues of the probe is prevented by hybrid formation at the bioelectrode surface, resulting in a much decreased signal compared with that from direct interaction with the nucleoside bases of single-stranded pDNA. The observed results demonstrate that the fabricated bioelectrode can be used to identify the target with high specificity.[34]

To examine the efficacy of the fabricated biosensor, the amperometric response in the presence of MB has been measured after hybridization with the target DNA at different concentrations. Figure 6A shows a decrease in the electrochemical signal with an increase in complementary DNA concentration, implying its applicability to perform quantitative pcDNA detection. The peak current value, pertaining to reduction of MB, exhibits a good linear relationship with the target nucleotide concentration in the range of 1.0 pM to 1.0 μM (Figure 6A, inset) and the correlation coefficient (R) in this range has been calculated to be as 0.9957 using the following equation:

$$I_{\mathrm{pDNA/CdTe/AS/ITO}}(A) = 1.0932 \times 10^{-5}(A) - 1.3392 \times 10^{-5}(A) \quad [\log(\text{target DNA concentration})] \tag{5}$$

The improved biosensing characteristics have been obtained for the fabricated biosensor compared to those of other DNA biosensors reported in literature for CML detection (Table 2).

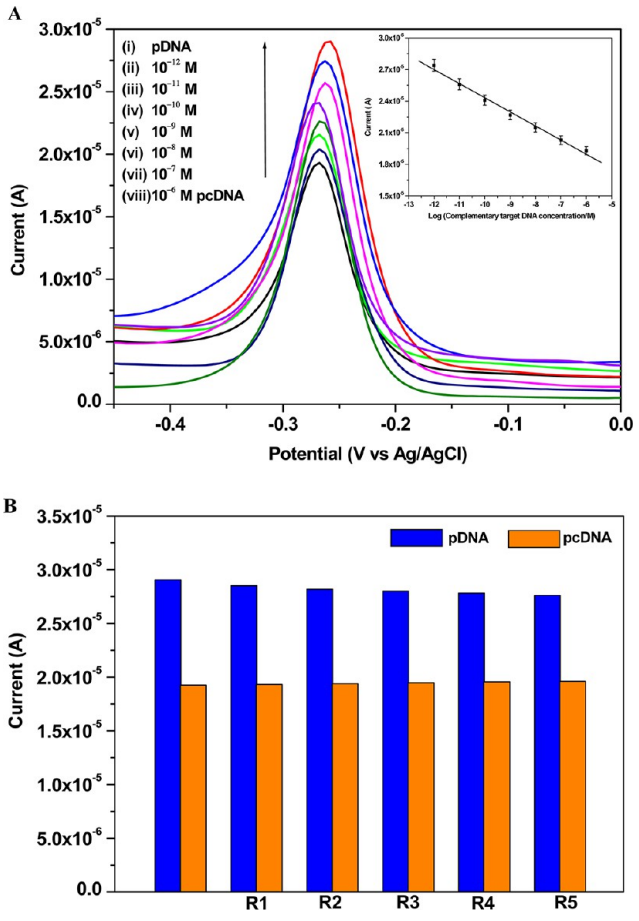

Figure 6. (A) Sensing characteristics of pDNA/CdTe/AS/ITO bioelectrode as a function of target DNA concentration in the range from 1 pM to 1 μM. The inset shows the linearity plot for the variation in MB peak height with respect to log of target DNA concentration. (B) Histogram showing variation in MB peak current of the pDNA/CdTe/AS/ITO bioelectrode with repeated cycling to hybridization and regeneration.

Table 2. Response Characteristics of pDNA/CdTe/AS/ITO Bioelectrode along with Those Reported in Literature for CML Detection

	RT-PCR results			
patient title	BCR copies	ABL copies	inference	biosensor inference
P1	20171	24490	CML +ve	CML +ve
P2	53796	68719	CML +ve	CML +ve
P3	3645	77101	CML +ve	CML −ve
P4	0	22873	CML −ve	CML −ve
P5	7451	28289	CML +ve	CML +ve

This may be attributed to the high charge detaching efficiency of CdTe-QDs that promote electron transfer from the electrode surface to pDNA molecules. These results are expected as CdTe-QDs provide high surface to volume ratio, thus increasing the effective surface area available for signal transduction and ultimately enhance the quantity of chemisorbed pDNA, leading to the improved detection limit.

Owing to the strong chemisorption of pDNA on the CdTe/AS/ITO electrode surface, the sensor is stable enough to allow for ready regeneration. For this, the electrode is immersed into a buffer solution (pH 8.0) containing Tris−HCl (10 mM) and EDTA (1 mM) at 100 °C for 5 min, followed by cooling in the ice bath for about 30 min, which completely removes hybridized DNA via thermal denaturation.[13,35] The MB peak current value of pDNA/CdTe/AS/ITO bioelectrode (0.290 μA) has been found to decrease after each regeneration process with an average signal loss from each hybridization cycle to be about 1% (Figure 6B), which may possibly be due to surface fouling while heating.[35,36] However, the ratio of DPV signal response after complementary binding versus pDNA/CdTe/AS/ITO bioelectrode remains almost constant. The total loss of hybridization signal after 5 cycles of hybridization/dehybridization is about 1.51 μA, and it corresponds to ∼5% of the initial value, indicating that the bioelectrode reproducibly detects target DNA over repeated uses. To investigate storage stability of the fabricated sensor, five measurements have been recorded each week for over 60 days of continuous analysis. The decrease in signal response of the bioelectrode is less than 8% when stored at 4 °C.

Prior to performing the electrochemical assay with PCR amplicons of BCR-ABL fusion gene, the samples are ultrasonicated to allow shearing. Gel electrophoresis experiment of the fragmented cDNA samples has been performed to obtain an estimation of fragments length with respect to sonication time (Figure 7A; panel i). The fragmentation profile is compared with the untreated probe DNA and hybridized DNA samples migrating as 22 bases and base pairs, respectively (Lane 4). Lane 1 sample shows low degree of fragmentation,

dx.doi.org/10.1021/la401431q | Langmuir 2013, 29, 8753−8762

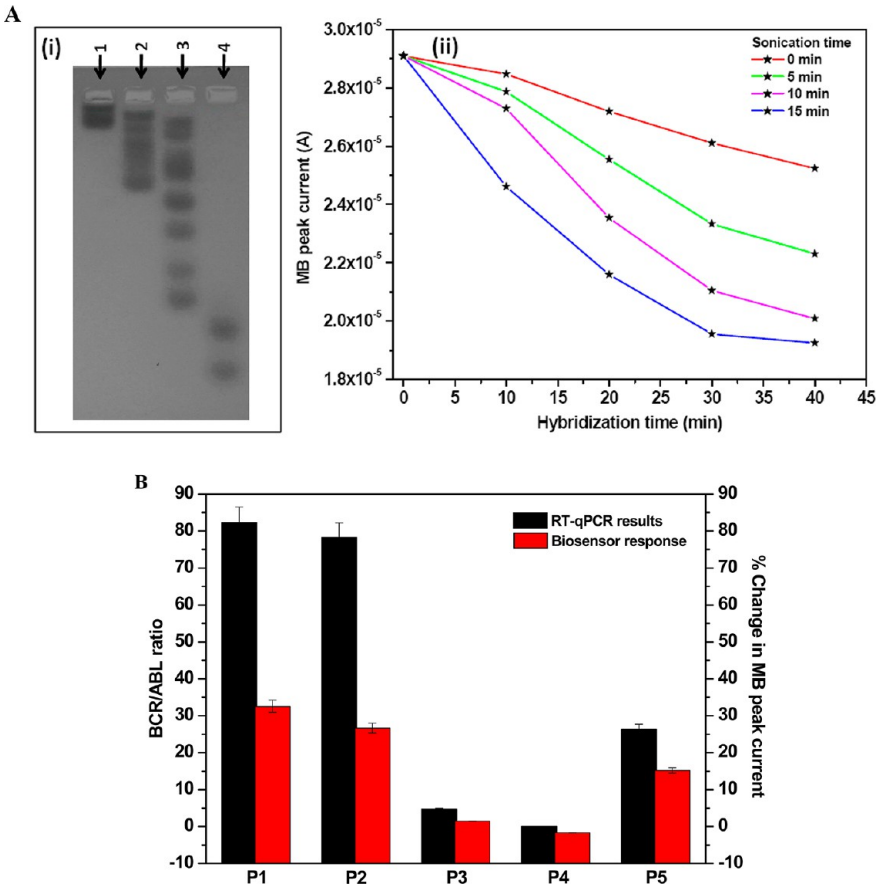

Figure 7. (A) (i) Agarose gel electrophoretogram showing fragmentation profile of PCR amplified real samples (Lanes 1 to 3) with respect to varying ultrasonication time; Lane 1: 5 min, Lane 2: 10 min, Lane 3: 15 min, and Lane 4: pDNA and pDNA + pcDNA corresponding to 22 and 44 bp ladders, respectively. (ii) Plot showing decrease in MB reduction current for pDNA/CdTe/AS/ITO bioelectrode as a function of hybridization time with PCR-amplified patient sample with respect to varying sonication time from 0 to 5 min. (B) Histogram presenting percentage variation in MB reduction value of the bioelectrode with respect to five different samples of both CML-negative and -positive patients with different BCR/ABL transcript ratios.

Table 3. Comparative Results of RT-PCR and Biosensing Assay for the Clinical Patient Samples

immobilization matrix	response time (min)	detection range (M)	limit of detection (M)	ref
amine terminated DNA/GCE	5	1.25×10^{-7} to 6.75×10^{-7}	5.9×10^{-8}	9
hairpin DNA/GCE	–	6.2×10^{-8} to 3.1×10^{-7}	5.3×10^{-9}	10
amine terminated DNA/GCE	30	2.0×10^{-7} to 2.0×10^{-8}	6.7×10^{-9}	11
amine terminated DNA/GCE	–	1.8×10^{-8} to 9.1×10^{-8}	6.7×10^{-9}	12
amine terminated DNA/CS-CdTe/ITO	1	1×10^{-6} to 1×10^{-11}	1×10^{-11}	13
thiol terminated DNA /QCdSe-SA-LB/ITO	2	1×10^{-6} to 1×10^{-14}	1×10^{-14}	14
pDNA/CdTe/AS/ITO	2	1×10^{-6} to 1×10^{-12}	1×10^{-12}	present work

however, with an increase in sonication period, the smaller fragments of cDNA are obtained (Lanes 2 and 3). It is also revealed that sonication produces unequal shearing of cDNA samples; however, fragmentation in the length range of about 50 bases is obtained after 15 min.

Figure 7A (panel ii) shows the variation in MB peak current value of the pDNA/CdTe/AS/ITO bioelectrode obtained as a function of hybridization time (0−40 min) with denatured and fragmented cDNA as a target. When the bioelectrode is incubated with cDNA without sonication, the MB peak current is found to remain almost constant, irrespective of the incubation period. With an increase in the sonication time (0−5 min) of the cDNA, the duplex formation is facilitated at the bioelectrode surface, as suggested by observed decrease in MB peak current value. The electrochemical studies have been performed with the fragmented cDNA samples, and the results are compared with the RT-PCR results to validate the sensor for clinical application. Figure 7B shows the comparative analysis of the results obtained from RT-PCR and biosensing assay for five different samples of both CML-negative and -positive patients, having BCR-ABL transcript levels ranging from 0 to 82% (as indicated by RT-PCR, Table 3). The electrochemical signal of MB reduction current significantly decreases after hybridization with the PCR-amplified positive real samples, having elevated levels of transcript, whereas negligible change in the value is obtained with positive real samples with low (~5%) BCR-ABL transcript ratio and with the negative patient sample. This reveals that the present biosensing assay is suitable for the detection of elevated levels

dx.doi.org/10.1021/la401431q | Langmuir 2013, 29, 8753−8762

of transcript. Experiments are underway to discern the exact copies of BCR/ABL, the sensor can precisely detect.

4. CONCLUSIONS

The present study is an important step toward the fabrication of a nucleic acid biosensor for detection of CML using QDs self-assembly based electrochemical assay. The QDs modified transducer surface is found to exhibit improved electron transfer kinetics compared to one without it. The designed synthetic CML specific capture probe, when covalently immobilized on the QDs modified surface, is found to specifically hybridize with its complementary DNA in the concentration range from 1 μM to 1 pM within 30 min. Its application in biological assay reveals that the sensing interface can qualitatively detect PCR amplified positive real samples with moderate to high BCR/ABL ratios, and thus presents an excellent prospect as an add-on technique toward initial screening of the disease. Efforts are underway to miniaturize the system into a hand-held device so as to enable point of care diagnostic of CML patients. Besides this, attempts should be made to improve the detection limit of this biosensor by using increased loading of probe DNA onto quantum dots based ordered molecular assembly obtained via Langmuir−Blodgett technique.

AUTHOR INFORMATION

Corresponding Author

*Tel: +91-11- 27871043; fax: +91-11-27871023; e-mail: bansi.malhotra@gmail.com.

Notes

The authors declare no competing financial interest.

ACKNOWLEDGMENTS

We thank the Director, NPL, New Delhi, India for the facilities. A.S. is thankful to CSIR, India, for the award of SRF. Thanks are due to Dr. Tathagat Chatterjee (Army Hospital, New Delhi) for providing the clinical patient samples along with RT-PCR data. We acknowledge the financial support received from the Department of Science & Technology (DST/TSG/ME/2008/18), Govt. of India, project], the in-house NPL project (OLP-070632D) and the Indian Council of Medical Research (ICMR/RHN/ADHOC/5/2012-2013). B.D.M. thanks the Ministry of Education, Science and Technology (*R*32−20026) of Korea for the opportunity provided during his visit to the Chungnam National University as Visiting Professor under the World Class University project during March−July 2013.

REFERENCES

(1) Sawyers, C. L. Chronic Myeloid Leukemia. *N. Engl. J. Med.* **1999**, *340*, 1330−1340.

(2) Clarkson, B.; Strife, A.; Wisniewski, D.; Lambek, C. L.; Liu, C. Chronic Myelogenous Leukemia As a Paradigm of Early Cancer and Possible Curative Strategies. *Leukemia* **2003**, *17*, 1211−1262.

(3) Nowell, P. C. Discovery of the Philadelphia Chromosome: A Personal Perspective. *J. Clin. Invest.* **2007**, *117*, 2033−2035.

(4) Druker, B. J.; Sawyers, C. L.; Kantarjian, H.; Resta, D. J.; Reese, S. F.; Ford, J. M.; Capdeville, R.; Talpaz, M. Activity of a Specific Inhibitor of the BCR-ABL Tyrosine Kinase in the Blast Crisis of Chronic Myeloid Leukemia and Acute Lymphoblastic Leukemia with the Philadelphia Chromosome. *N. Engl. J. Med.* **2001**, *344*, 1038−1042.

(5) Cortes, J. E.; Talpaz, M.; Kantarjian, H. Chronic Myelogenous Leukemia: A Review. *Am. J. Med.* **1996**, *100*, 555−570.

(6) Lee, W. I.; Kantarjian, H.; Glassman, A.; Talpaz, M.; Lee, M. S. Quantitative Measurement of BCR/abl Transcripts Using Real-Time Polymerase Chain Reaction. *Ann. Oncol.* **2002**, *13*, 781−788.

(7) Gooding, J. J. Electrochemical DNA Hybridization Biosensors. *Electroanalysis* **2002**, *14*, 1149−1156.

(8) Odenthal, K. J.; Gooding, J. J. An Introduction to Electrochemical DNA Biosensors. *Analyst* **2007**, *132*, 603−610.

(9) Lin, X.-H.; Wu, P.; Chen, W.; Zhang, Y.-F.; Xia, X.-H. Electrochemical DNA Biosensor for the Detection of Short DNA Species of Chronic Myelogenous Leukemia by Using Methylene Blue. *Talanta* **2007**, *72*, 468−471.

(10) Chen, J.; Zhang, J.; Wang, K.; Huang, L.; Lin, X.; Chen, G. Electrochemical Biosensor Based on Hairpin DNA Probe Using 2-Nitroacridone As Electrochemical Indicator for Detection of DNA Species Related to Chronic Myelogenous Leukemia. *Electrochem. Commun.* **2008**, *10*, 1448−1451.

(11) Chen, J.; Zhang, J.; Zhuang, Q.; Chen, J.; Lin, X. Hybridization Biosensor Using Sodium Tanshinone IIA Sulfonate As Electrochemical Indicator for Detection of Short DNA Species of Chronic Myelogenous Leukemia. *Electrochim. Acta* **2008**, *53*, 2716−2723.

(12) Chen, J.; Zhang, J.; Huang, L.; Lin, X.; Chen, G. Hybridization Biosensor Using 2-Nitroacridone As Electrochemical Indicator for Detection of Short DNA Species of Chronic Myelogenous Leukemia. *Biosens. Bioelectron.* **2008**, *24*, 349−355.

(13) Sharma, A.; Pandey, C. M.; Matharu, Z.; Soni, U.; Sapra, S.; Sumana, G.; Pandey, M. K.; Chatterjee, T.; Malhotra, B. D. Nanopatterned Cadmium Selenide Langmuir-Blodgett Platform for Leukemia Detection. *Anal. Chem.* **2012**, *84*, 3082−3089.

(14) Sharma, A.; Pandey, C. M.; Sumana, G.; Soni, U.; Sapra, S.; Srivastava, A. K.; Chatterjee, T.; Malhotra, B. D. Chitosan Encapsulated Quantum Dots Platform for Leukemia Detection. *Biosens. Bioelectron.* **2012**, *38*, 107−113.

(15) Hua, M.; Li, P.; Li, L.; Huang, L.; Zhao, X.; Feng, Y.; Yang, Y. Quantum Dots As Immobilized Substrate for Electrochemical Detection of Cocaine Based on Conformational Switching of Aptamer. *J. Electroanal. Chem.* **2011**, *662*, 306−311.

(16) Li, Y.; Han, M.; Bai, H.; Wu, Y.; Dai, Z.; Bao, J. A Sensitive Electrochemical Aptasensor Based on Water Soluble CdSe Quantum Dots (QDs) for Thrombin Determination. *Electrochim. Acta* **2011**, *56*, 7058−7063.

(17) Gaponik, N.; Talapin, D. V.; Rogach, A. L.; Hoppe, K.; Shevchenko, E. V.; Kornowski, A.; Eychmüller, A.; Weller, H. Thiol-Capping of CdTe Nanocrystals: An Alternative to Organometallic Synthetic Routes. *J. Phys. Chem. B* **2002**, *106*, 7177−7185.

(18) Xu, J.; Zhu, J.-J.; Huang, Q.; Chen, H.-Y. A Novel DNA-Modified Indium Tin Oxide Electrode. *Electrochem. Commun.* **2001**, *3*, 665−669.

(19) Fischer, M. J. Amine Coupling through EDC/NHS: A Practical Approach. *Methods Mol. Biol.* **2010**, *627*, 55−73.

(20) Yu, W. W.; Wang, Y. A.; Peng, X. Formation and Stability of Size-, Shape-, and Structure-Controlled CdTe Nanocrystals: Ligand Effects on Monomers and Nanocrystals. *Chem. Mater.* **2003**, *15*, 4300−4308.

(21) Oh, T. Correlation between Potential Barrier and FTIR Spectra in SiOC Film with the C−O Bond of sp^3 Structure. *Bull. Korean Chem. Soc.* **2009**, *30*, 468−470.

(22) Herreros, B.; Barr, T. L.; Barrie, P. J.; Klinowski, J. Spectroscopic Studies of 5-Coordinate Silicon Compounds. *J. Phys. Chem.* **1994**, *98*, 4570−4574.

(23) Chalmers, J. M.; Griffiths, P. R. *Handbook of Vibrational Spectroscopy*; Wiley: New York, 2002.

(24) Judith, R. M.; Rowena, R. G.; Tamara, M. J.; Susan, C.; Kurt, W. S.; Yujiro, R. Y.; James, P. F. Methods for Measuring the Infrared Spectra of Biological Cells. *Phys. Med. Biol.* **2003**, *48*, 243.

(25) Zoski, C. G. *Handbook of Electrochemistry*; Elsevier: Amsterdam/Boston, 2007.

(26) Laviron, E. General Expression of the Linear Potential Sweep Voltammogram in the Case of Diffusionless Electrochemical Systems. *J. Electroanal. Chem. Interfacial Electrochem.* **1979**, *101*, 19−28.

(27) Tang, L. H.; Wang, Y.; Li, Y. M.; Feng, H. B.; Lu, J.; Li, J. H. Preparation, Structure, and Electrochemical Properties of Reduced Graphene Sheet Films. *Adv. Funct. Mater.* **2009**, *19*, 2782−2789.
(28) Bard, A. J.; Faulkner, L. R. *Electrochemical Methods: Fundamentals and Applications*; Wiley: New York, 2000.
(29) Shi, J.; Claussen, J. C.; McLamore, E. S.; Haque, A. U.; Jaroch, D.; Diggs, A. R.; Calvo-Marzal, P.; Rickus, J. L.; Porterfield, D. M. A Comparative Study of Enzyme Immobilization Strategies for Multi-Walled Carbon Nanotube Glucose Biosensors. *Nanotechnology* **2011**, *22*, 355502.
(30) Li, J.; Liu, Q.; Liu, Y.; Liu, S.; Yao, S. DNA Biosensor Based on Chitosan Film Doped with Carbon Nanotubes. *Anal. Biochem.* **2005**, *346*, 107−114.
(31) Feng, L.; Wang, L.; Hu, Z.; Tian, Y.; Xian, Y.; Jin, L. Encapsulation of Horseradish Peroxidase into Hydrogel, And Its Bioelectrochemistry. *Microchim. Acta* **2009**, *164*, 49−54.
(32) Erdem, A.; Kerman, K.; Meric, B.; Ozsoz, M. Methylene Blue as a Novel Electrochemical Hybridization Indicator. *Electroanalysis* **2001**, *13*, 219−223.
(33) Kara, P.; Cavdar, S.; Meric, B.; Erensoy, S.; Ozsoz, M. Electrochemical Probe DNA Design in PCR Amplicon Sequence for the Optimum Detection of Microbiological Diseases. *Bioelectrochemistry* **2007**, *71*, 204−210.
(34) Pandey, C. M.; Singh, R.; Sumana, G.; Pandey, M. K.; Malhotra, B. D. Electrochemical Genosensor Based on Modified Octadecanethiol Self-Assembled Monolayer for *Escherichia coli* Detection. *Sens. Actuators B* **2011**, *151*, 333−340.
(35) Loaiza, Ó.; Campuzano, S.; López-Berlanga, M.; Pedrero, M.; Pingarrón, J. Development of a DNA Sensor Based on Alkanethiol Self- Assembled Monolayer-Modified Electrodes. *Sensors* **2005**, *5*, 344−363.
(36) Kang, D.; Zuo, X.; Yang, R.; Xia, F.; Plaxco, K. W.; White, R. J. Comparing the Properties of Electrochemical-Based DNA Sensors Employing Different Redox Tags. *Anal. Chem.* **2009**, *81*, 9109−9113.